Effects of band gap alignment and temperature on device performance of GaInP/Ga(In)As monolithic tandem solar cells

T. ATASER[a,b], N. AKIN[a], O. ZEYBEK[b], S. OZCELIK[a,c,*]
[a]*Photonics Application and Research Center, Gazi University, 06500, Ankara, Turkey*
[b]*Department of Physics, Faculty of Arts and Sciences, Balikesir University, 10145, Balikesir, Turkey*
[c]*Department of Physics, Faculty of Science, Gazi University, 06500, Ankara, Turkey*

In this study, $Ga_{1-y}In_yP/Ga_{1-x}In_xAs$ monolithic dual junction (DJ) solar cells (SCs) were designed and optimized using 0.00, 0.01, 0.05 and 0.30 values of Indium (In) content (x) for 0.58, 0.58, 0.62 and 0.72 values of (In) content (y), respectively. The short-circuit current density (J_{sc}), open-circuit voltage (V_{oc}) and conversion efficiency (η) of the four modeling SCs were numerically calculated. The band gaps were aligned to obtain the best performance of the cells by optimizing the content of (In) into layers in each cell. It was determined that the band gap of the cells decreased as increasing the (In) content both of (x) and (y), but the η of the SCs reduced accordingly. To obtain high η, it was suggested that the modeling $Ga_{1-y}In_yP/Ga_{1-x}In_xAs$ structure on GaAs substrate could be grown as inverted to realize low cost hybrid SCs or DJ thin film SCs on a flexible substrate. Furthermore, the band gap alignment effects the J_{sc}, V_{oc} and η of the SCs, as well as effect of the cell temperature on these parameters were also investigated. In addition, device performance of the SCs was also discussed under one-sun both AM1.5G and AM0 spectral conditions.

(Received May 16, 2016; accepted September 29, 2016)

Keywords: Modelling, DJ solar cells, Efficiency, Temperature dependence, AM1.5G and AM0 illumination

1. Introduction

Solar cells (SCs), also called photovoltaic cells are optoelectronic devices that can directly convert the sun's energy into electricity in the form of current and voltage by the photovoltaic effect discovered by the French scientist Henri Becquerel in 1839 [1-5]. III–V group-based SCs such as GaAs, InP and GaInP which are especially used in concentrator technology and for space applications [6,7]. These SCs can be designed at different architectures such as single junction (SJ), dual junction (DJ) and triple junction (TJ), etc. In multi-junction (MJ) SCs, interconnect in series of the cells is preferred to increase the output voltage and thereby the highest conversion efficiency of the SCs are obtained [8,9]. MJ SCs, which are sensitive to radiation of various wavelengths, consist of a stack of two or more junction SCs [10]. One top cell is selected from the materials with higher energy band gap, whereas a bottom cell is selected lower band gap materials. Whereby, bottom cell uses the photons which are not absorbed by the top cell of the structure [11,12].

III–V group compound semiconductors, such as GaInP, InGaN, InGaAsP and AlGaAs etc., are widely used as top cell materials of MJ SCs [13-15]. Among them, as one suitable candidate for the top cell material, GaInP has been demonstrated to be best option owing to its good material quality and appropriate energy band gap to absorb the visible part of the solar spectrum [4,16,17].

In the literature, there are several studies on improving of efficiency of the SCs under one-sun, AM1.5 global (AM1.5G), and concentrated illumination, called CPV, for terrestrial application and under AM0 illumination for space application. K.A. Bertness et al. reported that $Ga_{0.52}In_{0.48}P$/GaAs DJ SCs was %27.3 efficiency for AM1.5G and %25.7 efficiency for AM0 under one-sun [8]. For DJ SCs, in another study, GaInP/GaAs DJ SCs, lattice-matched to GaAs, have already proved that efficiencies over %29.5 for AM1.5G and %25.4 for AM0 spectral conditions, under one-sun [16]. The theoretical efficiency of GaInP/GaAs DJ SCs can be optimized with top cell thickness and energy band gap [18,19]. The highest theoretical efficiency of the GaInP/GaAs DJ SCs occurs when GaInP top cell is thinned to about 0.6 μm and its energy band gap about 1.86 eV [8,16,20]. Therefore, a sufficient part of the solar spectrum to produce photocurrent can pass into the GaAs bottom cell with 1.42 eV of band gap. In addition, theoretically higher efficiencies can be obtained by converting more of the infrared radiation of the solar spectrum with a lower energy band gap bottom cell [20]. To decrease the band gap of the bottom cell, it is a way of contains small amount of (In) of the structure. So, GaInP/Ga(In)As SCs are alternative structures to GaInP/GaAs SCs.

The compound semiconductors $Ga_{1-x}In_xAs$ have an energy band gap between 1.42 eV for GaAs and 0.35 eV for InAs. For instance, $Ga_{0.99}In_{0.01}As$ with a band gap energy of 1.405 eV can be grown lattice-matched to a GaAs substrate. Recently, several researchers have conducted studies on the growth of the lattice-matched $Ga_{1-x}In_xAs$ on GaAs substrates for the combination of optically active devices operating at different wavelengths

[21,22]. $Ga_{0.35}In_{0.65}P/Ga_{0.83}In_{0.17}As$ DJ SCs grown on GaAs substrates have already showed that efficiencies over %25.1 for AM1.5G and %21.6 for AM0 spectral conditions, under one-sun [22].

MJ SCs are affected under working condition such as cell temperature, wind speed, solar radiation intensity and characteristics of cooling system [23]. For instance, with the increase of the cell temperature, the energy band gap of the cell materials would decrease and so, the short-circuit current density slightly would increase while the open circuit voltage strongly decrease [24]. Recently, Singh and Ravindra calculated temperature effects on photovoltaic performance of SCs produced several materials [25].

III-V high efficiency MJ SCs has generally grown on germanium (Ge) substrate that has high cost cell materials. In recent years, hybrid TJ SCs have been built mechanical bonding with III-V DJ SCs and Si SCs [26, 27]. In this way, without lattice matching, low cost and high efficiency SCs can be fabricated. In this hybrid device architecture, the GaInAs/GaInP DJ SCs on GaAs substrate can be grown as inverted with selective etching layer. After the bonding, GaAs substrate can be removed by wafer lift-off process and it can be again used another SCs structure growth. In addition, using the epitaxial lift-off technique, the III-V DJ SCs can be transferred any substrate as well as flexible, to obtain epitaxial thin film SCs [28].

In our previous study, molecular beam epitaxy (MBE) grown GaInP/GaAs DJ SCs has performed with %13.52 conversion efficiency without antireflective coating under AM1.5G illumination [7]. In this experimental study, the band gap of GaInP and GaAs layers was 1.86 eV and 1.42 eV, respectively. It is known that the band gap of the bottom cell is sufficiently smaller; the SCs can produce more energy, especially, in TJ cells via the absorbing of the more part of the infrared region of the solar spectrum. In this presented study, we aimed to theoretically investigation of the effects on the conversion efficiency with band gap optimization of the cell structure via content of (In) into the layers in the cell structure. In this context, $Ga_{1-y}In_yP/Ga_{1-x}In_xAs$ DJ SCs which has (In) content (x) ranging from 0.00 to 0.30 and (In) content (y) ranging from 0.58 to 0.72 were designed by using analytical model of the SCs. The performance of each SCs is determined by current density-voltage (J-V) measurements. Firstly, short-circuit current density (J_{sc}), open-circuit voltage (V_{oc}) and conversion efficiency (η) of the $Ga_{1-y}In_yP/Ga_{1-x}In_xAs$ DJ SCs using 0.00, 0.01, 0.05 and 0.30 values of (In) content (x) for 0.58, 0.58, 0.62 and 0.72 values of (In) content (y) were calculated under one-sun AM1.5G and AM0 illuminations, respectively. Secondly, to understand the effect of the cell temperature on the parameters J_{sc}, V_{oc} and η of the $Ga_{1-y}In_yP/Ga_{1-x}In_xAs$ DJ SCs were calculated at different temperatures (200–400 K). We also discussed the results of under 300 sun AM1.5G condition for concentrating photovoltaic (CPV) technology.

2. Theoretical Approach

The device architecture of the $Ga_{1-y}In_yP/Ga_{1-x}In_xAs$ DJ SCs, which has a $Ga_{1-x}In_xAs$ bottom cell and $Ga_{1-y}In_yP$ top cell, are schematically represented in Fig. 1. In addition, this structure grown on GaAs substrate can be inverted to realize hybrid SCs or for transferring to any substrate using epitaxial lift-off technique. In this design, we considered two quantities to obtain current match for two junction SCs.

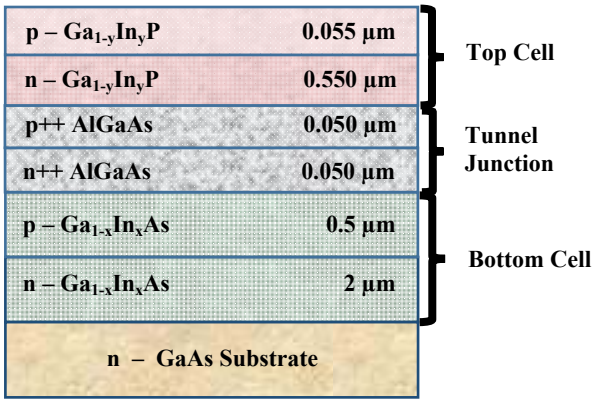

Fig. 1. The device architecture of the $Ga_{1-y}In_yP/Ga_{1-x}In_xAs$ DJ SCs

Firstly, the thickness and also doping concentration of the layers in each cells were determined as: $Ga_{1-x}In_xAs$ base is 2 µm thick with an n-type doping concentration of about $2x10^{17}$ cm^{-3} and $Ga_{1-x}In_xAs$ emitter is 0.5 µm thick with an p-type doping concentration of about $2x10^{18}$ cm^{-3}. For the $Ga_{1-y}In_yP$ top cell, its base is 0.55 thick with an n-type doping concentration of about $7x10^{17}$ cm^{-3} and its emitter is 0.05µm thick with an p-type doping concentration of about $2x10^{18}$ cm^{-3}. Secondly, the energy band gap was optimized by changing of the Indium (In) content into the layer in the each $Ga_{1-y}In_yP/Ga_{1-x}In_xAs$ DJ SCs as x=0, 0.01, 0.05, 0.30 and y=0.58, 0.58, 0.62, 0.72, respectively. These cells were named as SCs-1, SCs-2, SCs-3, SCs-4, respectively.

The energy band gap of the layers in the cells were calculated by using Vegard law ($E_{g_{Ga_{1-y}In_yP}}$=1.42+0.77(1-y)+0.648(1-y)^2 for top cells and $E_{g_{Ga_{1-x}In_xAs}}$=0.36+0.63(1-x)+0.43(1-x)^2 for bottom cells). Obtained band gaps were given in Table 1.

Table 1. Calculated energy band gaps of the $Ga_{1-y}In_yP/Ga_{1-x}In_xAs$ DJ SCs.

SCs	Top Cell E_g (eV)	Bottom Cell E_g (eV)
SCs-1	1.86	1.42
SCs-2	1.86	1.40
SCs-3	1.80	1.34
SCs-4	1.68	1.10

Electromagnetic radiation, including sunlight, is constituted of particles called photons. For the SCs, the absorption range of solar spectrum is defined by;

$$\lambda(\mu m) = \frac{1.24}{E_g(eV)} \quad (1)$$

Where λ is photon wavelength. If the incident photon energy is higher than the band gap energy (E_g) of the semiconductor, the photons are absorbed and electron-hole pair are generated in the cell [9,29]. The photogeneration of the carrier depends on the absorption coefficient (α) of the light in SCs material as well as initial photon flux (ϕ_0) [30]. The absorption coefficients of the GaAs, GaInAs and GaInP layers in the designed SCs structure, can be given as, respectively,

$$\alpha_{GaAs}(\lambda) = 3.3\sqrt{(E - E_g)} \quad (2)$$

$$\alpha_{Ga_{1-x}In_xAs}(\lambda) = 3.3\sqrt{(E - E_g)} \quad (3)$$

$$\alpha_{Ga_{1-x}In_{xP}}(\lambda) = 5.5\sqrt{(E - E_g)} + \\ +1.5\sqrt{(E - E_g - 0.1)}. \quad (4)$$

Where E is the photon energy and E_g the fundamental energy gap, both in eV, and α in 1/μm [19,29].

The wavelength integral of the short-circuit density current of the SCs;

$$J_{sSC}(\lambda) = \int_0^{\infty} J_{sc\lambda} d\lambda = \int_0^{\infty} (J_{scE} + J_{scB}) d\lambda. \quad (5)$$

Where J_{scE}, J_{scB}, emitter and base short-circuit current density, respectively. Emitter and base short-circuit current density of the SCs are given as, respectively, [31];

$$J_{SCE}(\lambda) = \frac{q\alpha\phi_0(1-R)L_p}{(\alpha L_p)^2 - 1} \left[-\alpha L_p e^{-\alpha W_e} \right. \\ \left. + \frac{S_e \frac{L_p}{D_p} + \alpha L_p - e^{-\alpha W_e}\left(S_e \frac{L_p}{D_p} cosh\frac{W_e}{L_p} + sinh\frac{W_e}{L_p}\right)}{cosh\frac{W_e}{L_p} + S_e \frac{L_p}{D_p} sinh\frac{W_e}{L_p}} \right] \quad (6)$$

$$J_{SCB}(\lambda) = \frac{q\alpha\phi_0'(1-R)L_n}{(\alpha L_n)^2 - 1} \left[-\alpha L_n \right. \\ \left. - \frac{S_b \frac{L_n}{D_n}\left(cosh\frac{W_b}{L_n} - e^{-\alpha W_b}\right) + sinh\frac{W_b}{L_n} + \alpha L_n e^{-\alpha W_b}}{cosh\frac{W_b}{L_n} + S_b \frac{L_n}{D_n} sinh\frac{W_b}{L_n}} \right] \quad (7)$$

Where $D_{n,p} = \mu_{n,p} {}^{kT}/_{q}$ [18], $\tau_{n,p} = [{}^{1}/_{BN}]$ and $L_{n,p} = \sqrt{\tau_{n,p} D_{n,p}}$ [32].

Emitter and base saturation current density of the SCs are given as, respectively, [31];

$$J_{0E} = q\frac{n_i^2}{N_D}\frac{D_p}{L_p}\left[\frac{\left(S_e \frac{L_p}{D_p} cosh\frac{W_e}{L_p} + sinh\frac{W_e}{L_p}\right)}{cosh\frac{W_e}{L_p} + S_e \frac{L_p}{D_p} sinh\frac{W_e}{L_p}}\right] \quad (8)$$

$$J_{0B} = q\frac{n_i^2}{N_A}\frac{D_n}{L_n}\left[\frac{\left(S_b \frac{L_n}{D_n} cosh\frac{W_b}{L_n} + sinh\frac{W_b}{L_n}\right)}{cosh\frac{W_b}{L_n} + S_b \frac{L_n}{D_n} sinh\frac{W_b}{L_n}}\right] \quad (9)$$

Where $n_i = \sqrt{N_A N_D} e^{-{}^{E_g}/_{2kT}}$ [18] is used and saturation density current of the SCs is given $J_0 = J_{0e} + J_{0b}$, q is the electron charge, ϕ_0 is photon spectral flux at the emitter surface, ϕ_0' is photon spectral flux at the base-emitter interface, α is the optical absorption coefficient, and R is reflection coefficient, n_i is the intrinsic carrier concentration, and N_A and N_D are the concentrations of acceptors and donors. W_e and W_b are the emitter and base thickness, respectively. L_p is the hole diffusion length in the emitter, and L_n is the electron diffusion length in the base. S_e and S_b are the hole and electron surface recombination velocity in the emitter and the base, respectively.

J-V characteristic of the SCs is given by

$$J = J_{sc} - J_0\left(e^{\frac{qV}{kT}} - 1\right) \quad (10)$$

The open-circuit voltage is the maximum voltage available from the SCs. Equation (10) at J=0 yields the expression for V_{oc} as;

$$V_{oc} = \frac{kT}{q}\ln\left(\frac{J_{sc}}{J_0} + 1\right) \quad (11)$$

As a consequence of the temperature variation, the band gap energy changes according to the equation giving by Varshni [33];

$$E_g(T) = E_g(0) - \frac{\alpha T^2}{T + \beta} \quad (12)$$

Where $E_g(0)$ is the energy band gap at T= 0 °K, T is the absolute temperature in Kelvin, and α and β are the coefficients which are characteristic of a given semiconductor.

Fill factor (FF) of the SCs is the ratio of the maximum power from the cell to the product of Voc and Jsc as $P_{max}/V_{oc}J_{sc}$. However, FF can be calculated using below equation defined by Green [34];

$$FF = \frac{\upsilon_{oc} - \ln(\upsilon_{oc} + 0{,}72)}{1 + \upsilon_{oc}} \quad (13)$$

Where, $\upsilon_{oc} = qV_{oc}/kT$ is "normalized V_{oc}".
Efficiency of a SCs as depending on the fill factor can be calculated using the following relationship:

$$\eta = FF\frac{V_{oc}I_{sc}}{P_{in}} \qquad (14)$$

where, P_{in} is the intensity of the incident solar radiation. The parameters that are used to calculation of the quantities described in above equations were listed in Table 2.

Table 2. The parameters that are used to calculation for output of the PV cells.

Symbol	$Ga_{1-x}In_xAs$				GaInP
	x=0	x=0.01	x=0.05	x=0.30	
$\mu_n(cm^2/Vs)$*	8500	8327	7738	7618	4000
$\mu_p(cm^2/Vs)$*	400	200	200	200	200
$B_{n,p}(cm^3/s)$*	7.50 x10^{-10}	9.60 x10^{-11}	9.60 x10^{-11}	9.60 x10^{-11}	7.50 x10^{-10}
$Dn(cm^2/s)$	219.93	215.46	200.22	197.11	103.5
$Dp(cm^2/s)$	10.35	5.175	5.175	5.175	5.175
L_n(cm)	1.21 x10^{-3}	3.35 x10^{-3}	3.23 x10^{-3}	3.2 x10^{-3}	4.44 x10^{-04}
L_p(cm)	8.31 x10^{-5}	1.64 x10^{-4}	1.64 x10^{-4}	1.64 x10^{-4}	5.87 x10^{-05}
$S_{n,p}$ (cm/s)*	5000	8x10^4	1x10^5	1x 10^5	1x10^6

*Taken from Ref [35].

3. Results

Short-circuit current density (J_{sc}), open-circuit voltage (V_{oc}) and conversion efficiency (η) of the four modeling $Ga_{1-y}In_yP/Ga_{1-x}In_xAs$ DJ SCs (x=0, 0.01, 0.05 0.30 and y= 0.58, 0.58, 0.62 and 0.72, respectively) were calculated under AM1.5G and AM0 at 300 K. To evaluate the current matching of each SCs, obtained J-V variation of the bottom and top cells separately and together cells as device for every (In) content (x) and (y) values were presented in Fig. 2. As seen in this figure, the bottom and top cells which are DJ cells built up with their monolithic combination, are nearly current match. In addition, J_{sc} of the top cells in each DJ cells is slightly lower than the bottom cells. This means that the J_{sc} of the DJ device is limited by the top cell.

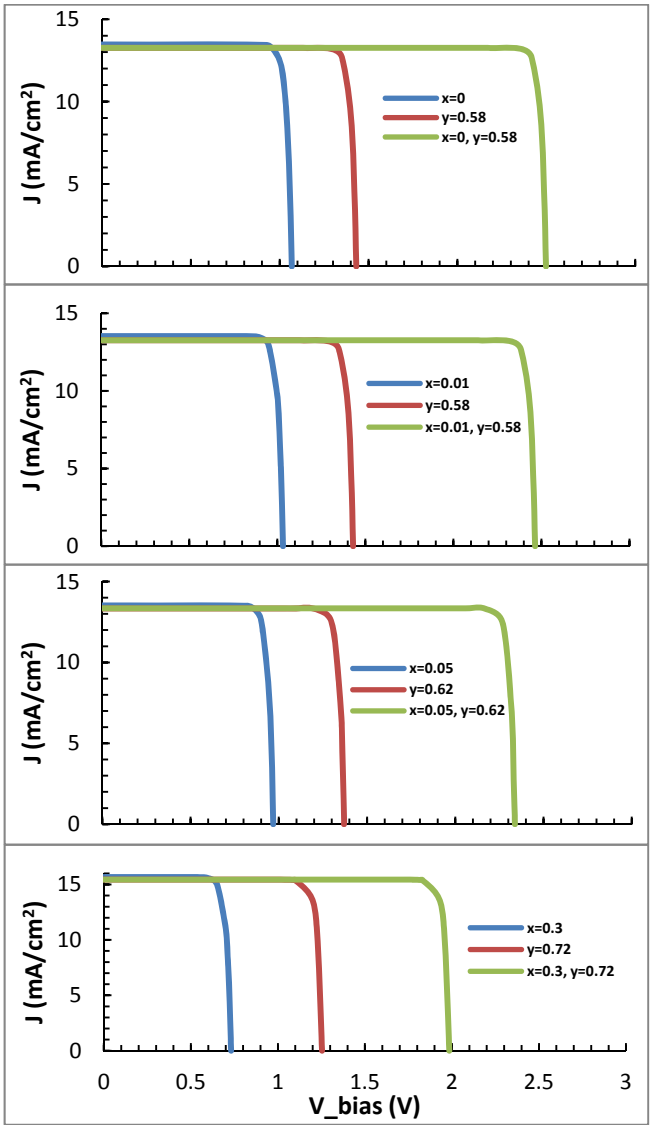

Fig. 2. Current match of the bottom cells, top cells and $Ga_{1-y}In_yP/Ga_{1-x}In_xAs$ DJ SCs

Comparison of the four devices, J–V characteristics of the $Ga_{1-y}In_yP/Ga_{1-x}In_xAs$ DJ SCs under AM1.5G at 300 K were detailed shown in Fig. 3. It was seen from the graphed figures that the J_{sc}, calculated based on Eq. (5, 6 and 7), increased with increasing the (In) content both (x) and (y) of the SCs layers. For AM1.5G, the J_{sc} of $Ga_{0.42}In_{0.58}P/GaAs$(SCs-1), $Ga_{0.42}In_{0.58}P/Ga_{0.99}In_{0.01}As$(SCs-2),$Ga_{0.38}In_{0.62}P/Ga_{0.95}In_{0.05}As$ (SCs-3) and $Ga_{0.28}In_{0.72}P/Ga_{0.7}In_{0.3}As$ (SCs-4) DJ SCs are 13.26, 13.26, 13.91 and 15.43 mA/cm^2, respectively. For AM0, the J_{sc} of these SCs were calculated as 17.16, 17.16, 17.25 and 18.19 mA/cm^2, respectively. In addition, increasing of (In) content in the SCs has led to a remarkable reduction in V_{oc}. For instance, when (In) content was increased from 0.0 to 0.3, the V_{oc} was decreased 2.5 to 2.0 V.

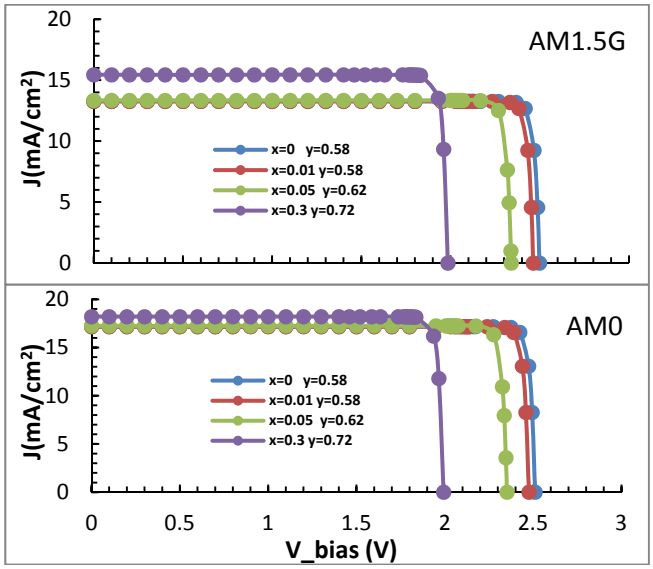

Fig. 3. J_{sc} versus V_{oc} of the $Ga_{1-y}In_yP/Ga_{1-x}In_xAs$ DJ SCs

The output parameters of the $Ga_{1-y}In_yP/Ga_{1-x}In_xAs$ DJ SCs under 1-sun and 300-sun for AM1.5G and 1-sun for AM0 radiation using above (In) content (x) and (y) values were given in Table 3. When the (x) and (y) value in the SCs layers increased, the V_{oc} decreased although the J_{sc} minimally increased. These results are associated with a lower band gap as increasing the (x) and (y) value of the SCs layers. The decrease in η is mainly controlled by the decrease of V_{oc}, while increase in J_{sc} does not affect η [36]. The η of the each SCs structure was increased about 12.6% under 300-sun, as seen in the last two column in Table 3. For instance, the η of $Ga_{0.42}In_{0.58}P$/GaAs DJ SCs has reached 35.11% under 300-sun radiation.

Table 3. The theoretically calculated J_{sc}, V_{oc} and η of the SCs

SCs	J_{sc} AM 1.5	J_{sc} AM0	V_{oc} AM1.5	V_{oc} AM0	η (%) AM0 (1x)	η (%) AM1.5 (1x)	η (%) AM1.5 (300x)
SCs-1	13.26	17.16	2.49	2.51	30.04	31.24	35.11
SCs-2	13.26	17.16	2.46	2.47	29.60	30.78	34.64
SCs-3	13.91	17.25	2.33	2.35	28.19	29.30	33.25
SCs-4	15.43	18.19	1.98	1.99	26.96	28.53	33.04

External quantum efficiencies (EQE) of a PV cells is related with the ratio of the J_{sc} and the initial photon flux ($q\phi_0$): EQE = Jsc/$q\phi_0(\lambda)$, where q is electron charge. In Fig. 4, calculated EQE of $Ga_{1-y}In_yP/Ga_{1-x}In_xAs$ DJ SCs under AM1.5G has indicated that top cells have generated the current from 300 nm to 630, 630, 650 and 690 nm for y=0.58, 0.58, 0.62 and 0.72, respectively. The photocurrent generation of the bottom cells started at 630 nm, 630 nm, 650 nm and 670 nm and terminated at 860 nm, 890 nm, 925 nm and 1120 nm for x= 0, 0.01, 0.05 and 0.30, respectively. The cut-off wavelength (λ(nm) = 1240/Eg(eV)) of the cells was increased with values of (x) and (y) and total area under the EQE curves increased with incorporation of (In) into the cell structures. Result of this, the J_{sc} also increased. However, the η of the SCs decreased due to V_{oc} decreased with lower band gap when increasing of (In) incorporation into the cells.

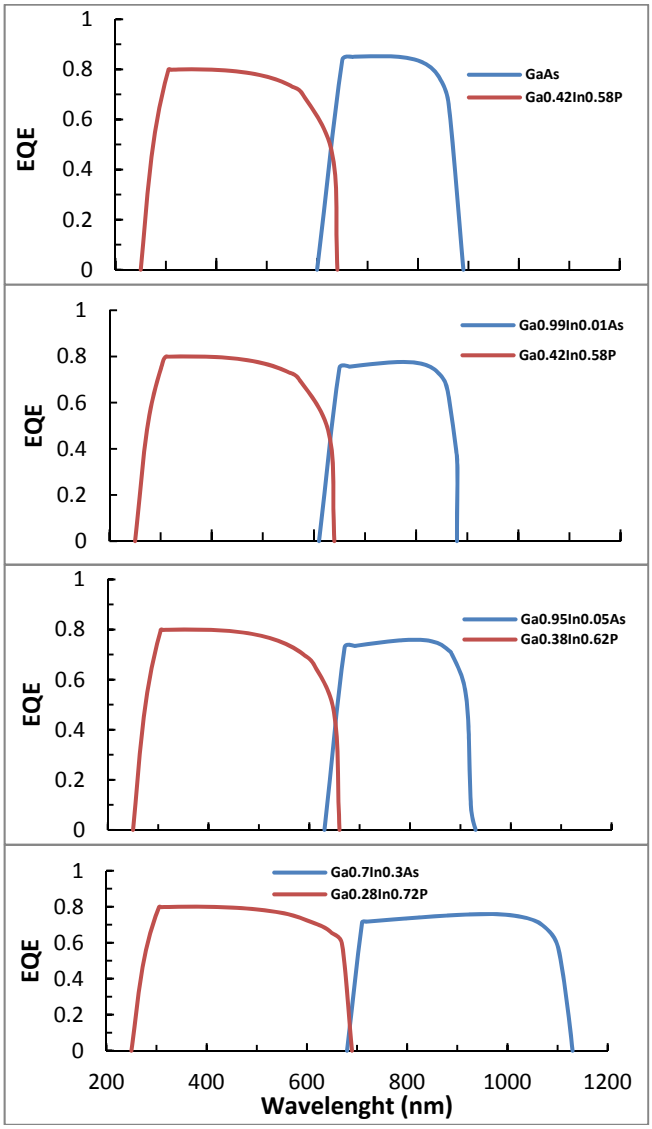

Fig. 4. EQE of $Ga_{1-y}In_yP/Ga_{1-x}In_xAs$ DJ SCs under AM1.5G

In this study, it was also aimed to investigate cell temperature effects on the output parameters (J_{sc}, V_{oc} and η) of the $Ga_{1-y}In_yP/Ga_{1-x}In_xAs$ DJ SCs. The parameters of the DJ SCs were calculated as a function of the cell temperature, with changing between 200–400 K. J_{sc} of the SCs mainly depends on the optical absorption coefficient (α(λ)) which relies on the energy gap (E_g) of the semiconductor materials [37], as seen in Eqs.(6 and 7). In addition, increasing of temperature will make narrower E_g of the SCs that will widen the optical absorption coefficient slightly across the spectrum [37-39]. Thus, the more photon-generated carriers will be produced, which results of the increase of J_{sc}. Consequently, J_{sc} is approximately proportional to the incident spectral intensity at wavelength near the band edge [6].

Fig. 5 shows the J_{sc} of the $Ga_{1-y}In_yP/Ga_{1-x}In_xAs$ DJ SCs for AM1.5G and AM0, depending on the temperature.

It was seen that the J_{sc} of the devices increased with increasing the temperature, as expected.

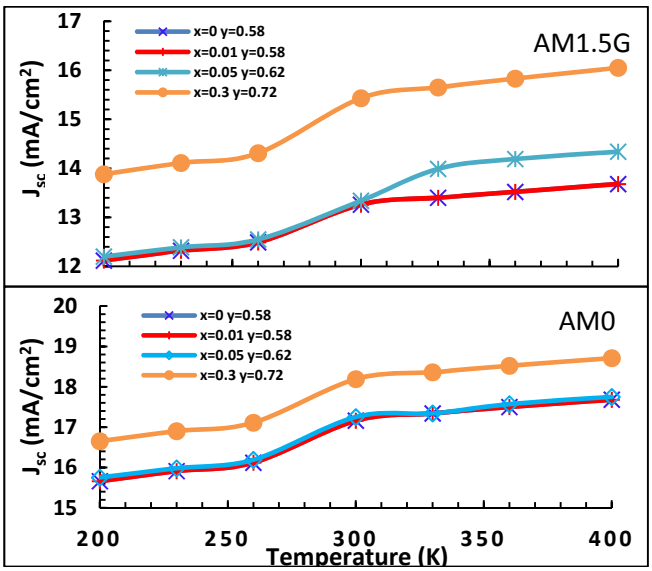

Fig. 5. J_{sc} of the $Ga_{1-y}In_yP/Ga_{1-x}In_xAs$ DJ SCs for AM1.5G and AM0, depending on the temperature

Fig. 6 shows that the V_{oc} of the $Ga_{1-y}In_yP/Ga_{1-x}In_xAs$ DJ SCs for AM1.5G and AM0 at different temperatures. V_{oc} was determined from the calculated J_{sc} and J_o using Eq.(11). The V_{oc} linearly decreased when the temperature of SCs increased. Due to the decreasing in V_{oc} was higher than the increasing in J_{sc}, it can be said that the high temperature has a negative impact on SCs performance.

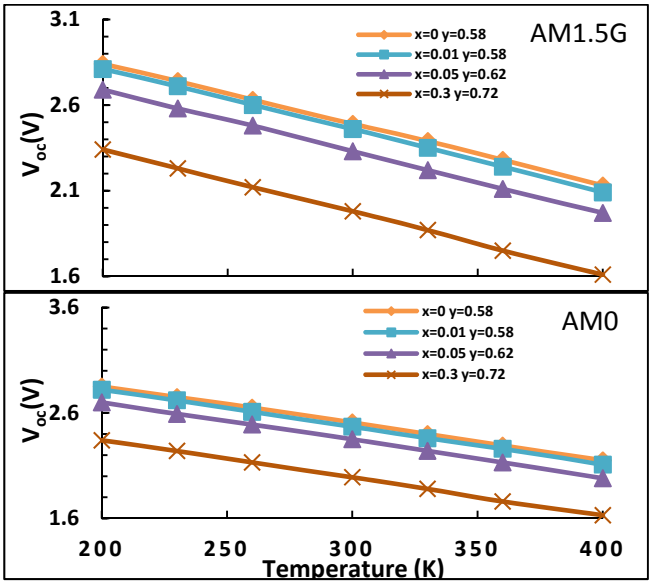

Fig. 6. V_{oc} of the $Ga_{1-y}In_yP/Ga_{1-x}In_xAs$ DJ SCs for AM1.5G and AM0, depending on the temperature

Fig. 7 shows that the η of the $Ga_{1-y}In_yP/Ga_{1-x}In_xAs$ DJ SCs for AM1.5G and AM0 at different temperatures. The η was calculated by using Eq.(14) corresponding to the obtained V_{oc} and J_{sc} at each temperature. When the temperature of SCs increased from 200 to 400 K, the voltage, V_{oc}, decreased although the current density, J_{sc} increased. Since the V_{oc} decreases faster than the J_{sc} increases, so the η goes down.

Therefore, the efficiency, η, increased at the temperatures below 300 K although it decreased at higher temperatures than 300 K, as seen in Fig. 7. Similar behavior for the GaAs solar cell output parameters depends on the temperature was determined by Sign and Ravindra [25].

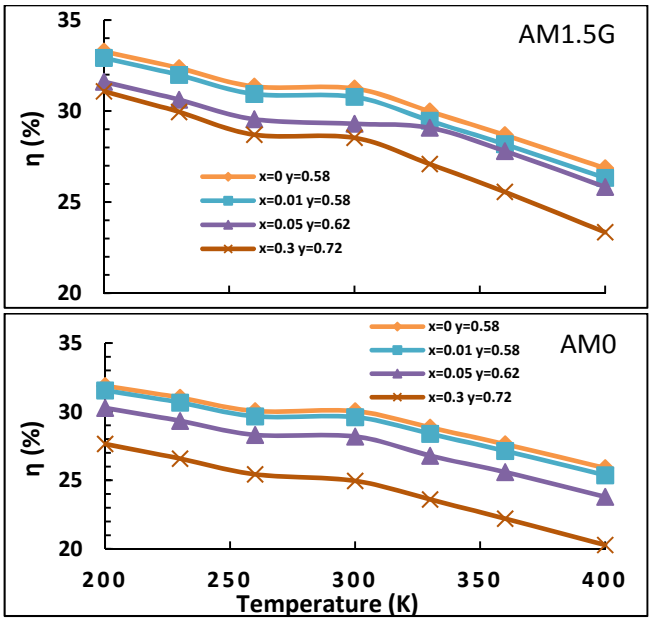

Fig. 7. η of the $Ga_{1-y}In_yP/Ga_{1-x}In_xAs$ DJ SCs for AM1.5G and AM0 , depending on the temperature

The performances of the SCs at 200, 300 and 400 K were compared in Table 4 for investigation of high temperature effects on the $Ga_{1-y}In_yP/Ga_{1-x}In_xAs$ DJ SCs for AM1.5G and AM0 spectra. As seen in Table 4, the J_{sc} and V_{oc} of the devices for AM0 are higher than AM1.5G due to the incident power which was known as 1353 Wm^{-2} and 1000 Wm^{-2} in the AM0 and AM1.5G conditions, respectively. In contrary, obtained SCs efficiencies for AM1.5G were slightly higher than for AM0 and this difference in efficiency may be attributed to incident power [6].

Table 4. Performance of the $Ga_{1-y}In_yP/Ga_{1-x}In_xAs$ DJ SCs

T (K)	SCs	J_{sc} AM1.5	J_{sc} AM0	V_{oc} AM1.5	V_{oc} AM0	η(%) AM1.5	η(%) AM0
200	SCs-1	12.12	15.66	2.84	2.85	33.27	31.88
	SCs-2	12.12	15.66	2.81	2.82	32.92	31.55
	SCs-3	12.20	15.75	2.69	2.70	31.61	30.27
	SCs-4	13.88	16.65	2.34	2.34	31.08	27.65
300	SCs-1	13.26	17.16	2.49	2.51	31.24	30.04
	SCs-2	13.26	17.16	2.46	2.47	30.78	29.60
	SCs-3	13.34	17.25	2.33	2.35	29.33	28.19
	SCs-4	15.43	18.19	1.98	1.99	28.53	24.96
400	SCs-1	13.68	17.68	2.13	2.15	26.86	25.90
	SCs-2	13.68	17.68	2.09	2.11	26.33	25.37
	SCs-3	14.34	17.75	1.97	1.98	25.83	23.80
	SCs-4	16.05	18.71	1.61	1.63	23.35	20.29

4. Conclusions

$Ga_{1-y}In_yP/Ga_{1-x}In_xAs$ monolithic tandem SCs architectures were designed by band gap optimization with arranging the content of indium (In) atoms in bottom and top cells. The short-circuit current density (J_{sc}), open-circuit voltage (V_{oc}) and conversion efficiency (η) were theoretically calculated depend on band gap variation each layer or content of (In) into the layers under AM1.5G and AM0 illuminations. Maximum SCs conversion efficiency as well as current matched structure were obtained for x= 0.00, 0.01, 0.05 and 0.30 and y= 0.58, 0.58, 0.62 and 0.72, respectively. For one- sun AM1.5G in terrestrial applications, the η values of $Ga_{0.42}In_{0.58}P/GaAs$, $Ga_{0.42}In_{0.58}P/Ga_{0.99}In_{0.01}As$, $Ga_{0.38}In_{0.62}P/ Ga_{0.95}In_{0.05}As$ and $Ga_{0.28}In_{0.72}P/Ga_{0.7}In_{0.3}As$ DJ SCs were obtained as %31.24, %30.78 %29.30 and %28.53, respectively. The efficiency of the each SCs was increased about 12.6% under 300-sun. For AM0 in space application, the η values of the same structures were calculated as %30.04, %29.60, %28.19 and %26.96, respectively. In addition, $Ga_{1-y}In_yP/Ga_{1-x}In_xAs$ DJ SCs output parameters based on the temperature were investigated in the range of 200–400 K. The J_{sc} slightly increased and V_{oc} strongly decreased, so the performance of the SCs decreased with increasing temperature.

We believe that this presented studies on the optimization of the $Ga_{1-y}In_yP/Ga_{1-x}In_xAs$ DJ SCs with different (In) content are guiding on epitaxially growth of the monolithic DJ SCs structure with current matching as well as lattice match with GaAs substrate. Besides for this, the designed SCs can be used to produce hybrid TJ SCs by mechanical integration or bonding to any SCs that have lower band gap energy than bottom cells in the designed SCs. In addition, for producing of low cost DJ SCs, the designed cells can be transferred to low cost substrate than GaAs such as Si by epitaxial lift-off technique. For this technique, the cell structure can be grown on GaAs substrate as an inverted and, after the bonding; the substrate can be reused for growth to another cell structure. By using this procedure, the designed DJ SCs can also be bond on any flexible substrate to produce low cost III-V monocrystalline thin film SCs such as thin stainless steel sheet or plastic substrate. This type SCs can be preferred to produce energy in air and space vehicles owing to their lightweight and high PV conversion efficiency.

Acknowledgements

This study was supported by Ministry of Development and Tubitak under Project Numbers 2011K120290 and 118T333, respectively.

References

[1] L. Castafier, S. Silvestre, Universidad Politecnica de Catalunya, John Wiley&Sons, 1–3 (2002).
[2] K. Tanabe, Energies **2**, 504 (2009).
[3] P. Hersch, K. Zweibel, Technical Information Office, 7–8 (1982).
[4] B. Kinaci, Y. Ozen, S.S. Cetin, T. Memmedli, M. Kasap, S. Ozcelik, J Mater Sci: Mater Electron **24**, 3269 (2013).
[5] Stephen J. Fonash, Solar Cell Device Physics, 2nd Edition, Academic Press 1-2 (2010).
[6] P. Singh, N.M Ravindra, Solar Energy Materials & Solar Cells **101,** 36 (2012).
[7] Y. Ozen, N. Akin, B. Kinaci, S. Ozcelik, Solar Energy Materials & Solar Cells **137,** 1 (2015).
[8] K. A. Bertness, D. J. Friedman, A.E. Kibbler, C. Kramer, R. Kurtz Sarah, J. M. Olson, AIP Conference Proceedings **306,** 100 (1994).
[9] S. Sheik Mohammed, IJCEE **5,** 350 (2011).
[10] M. Cooke, Compd. Adv. Silicon **7,** 72 (2013).
[11] A. Morales-Acevedo, G. Casados-Cruz, International Journal of Photoenergy 1–5 (2013).
[12] S.M. Bedair, M.F. Lamorte, J. R. Hauser, Appl. Phys. Lett. **34**, 38 (1979).
[13] J.M. Roman, Advanced Photovoltaic Cell Design 1–8 (2004).
[14] S.W. Feng, C.M. Lai, C.Y. Tsai, L.W. Tu, Nanoscale Research Letters **9**(652), 1 (2014).
[15] M. Yamaguchi, T. Takamoto, K. Araki, N. Ekins-Daukes, Solar Energy **79,** 78 (2005).
[16] K.A. Bertness, R. Kurtz Sarah, D.J. Friedman, A.E Kibbler, C. Kramer, J.M. Olson, Appl Phys Letters **65**, 989 (1994).
[17] I. Garcia, I. Rey-Stolle, B. Galiana, C. Algora, Appl Phys Lett **94**(053509), 1 (2009).
[18] R. Kurtz Sarah, P. Faine, J.M. Olson, J. Appl. Phys. **68**, 1890 (1990).
[19] J.M. Olson, R. Kurtz Sarah, A.E. Kibbler, P. Faine, Applied Physics Letters **56,** 623 (1990).
[20] F. Dımroth, P. Lany, U. Schubert, A.W. Bett, Journal of Electronic Materials **29,** 42 (2000)
[21] F. Dimroth, U. Schubert, A.W. Bett, IEEE Electron Device Letters **21,** 209 (2000).
[22] C. Lobo, R. Leon, Journal of Applied Physics **83,** 4168 (1998).
[23] Z. Wang, H. Zhang, W. Zhao, Z. Zhou, M. Chen, The Open Fuels & Energy Science Journal **8**, 106 (2015).
[24] A. Laudani, F. Mancilla-David, F. Riganti-Fulginei, A. Salvini, Solar Energy **97**, 122 (2013).
[25] Singh P. and Ravindra N.M. Solar Energy Materials and Solar Cells **101**, 36 (2012)
[26] K. Derendorf, S. Essig, E. Oliva, V. Klinger, T. Roesener, S. P. Philipps, et al. IEEE J. Photovoltaics **3,** 1423 (2013).
[27] J. Yang, Z. Peng, D. Cheong, R. Kleiman, IEEE J. Photovoltaics **4** 149 (2014).
[28] C. Youtsey, J. Adams, R. Chan, V. Elarde, G. Hillier, M. Osowski, D. McCallum, H. Miyamoto, N. Pan, C. Stender, et al. CS Mantech Conference 1–4, (2012).
[29] A. Luque, S. Hegedus, Handbook of Photovoltaic Science and Engineering, John Wiley & Sons p. 61–62, 2002.

[30] S. M. Sze John, Physics of Semiconductor Devices, Wiley & Sons p. 264, 727 1981.
[31] L. Guijiang, W. Jyhchiarng, H. Meichun, Journal of Semiconductors **31,** 1 (2010).
[32] Z. Han, C. Nuofu, W. Yu, Y. Zhigang, Z. Xingwang, S. Huiwei, W. Yanshuo, H. Tianmao, Journal of Semiconductors, **31,** 1 (2010).
[33] M.B, Panish, H.C Casey Jr., Journal of Applied Physics **40,** 163 (1969).
[34] M.A. Green, Solar Cells, Prentice-Hall, Englewood Cliffs, NJ, p. 88, 1982.
[35] Web: http://www.ioffe.ru/SVA/NSM/Semicond/
[36] P. Singh, S.N. Singh, M. Lal, M. Husain, Solar Energy Materials& Solar Cells **92,** 1611 (2008).
[37] C. Min, C. Nuofu, Y. Xiaoli, Z. Han, Journal of Semiconductors **33,** 1 (2012).
[38] A. Green Martin, Prog. Photovolt: Res. Appl. **11**, 333 (2003).
[39] L. Lei, C. NuoFu, B. YiMing, C. Ming, Z. Han, G. FuBao, Y. ZhiGang, Z. XingWang, Science in China Series E: Technological Sciences **52,** 1176 (2009).

*Corresponding author: sozcelik@gazi.edu.tr